PHYSICAL REVIEW A VOLUME 26, NUMBER 4 OCTOBER 1982

Theory of two-photon optical tristability

J. A. Hermann
Optics Section, The Blackett Laboratory, Imperial College, London, SW7 2AZ, England

D. F. Walls
Department of Physics, University of Waikato, Hamilton, New Zealand
(Received 23 November 1981)

An intracavity two-photon absorber interacting with two coherently driven cavity modes is studied. The possible stable output configurations of the cavity-mode amplitudes are determined for both the absorptive and dispersive cases. Under certain conditions this system is shown to display optical bi- and tristability.

I. INTRODUCTION

The possibility of realizing multistable transmission characteristics using a resonator supporting two or more modes of the electromagnetic field interacting through a nonlinear medium has been discussed very recently by Kitano *et al.*,[1] Hermann *et al.*,[2,3] and Walls *et al.*[4,5] Using a rate-equation approach Kitano *et al.*[1] have shown that optical tristability may result from a system of three-level atoms inside an optical cavity driven with linearly polarized light. New bifurcation phenomena may occur using a different nonlinear medium as discussed by Walls *et al.*[4,5] In this paper we wish to discuss in detail the behavior of an intracavity two-photon absorber interacting with two cavity modes. Such a coherently driven cavity interacting with only one mode of the radiation field was analyzed theoretically (Arecchi and Politi[6]) and bistable behavior was predicted. This two-photon optical bistability was realized experimentally by Giacobino *et al.*[7] When the two photons are absorbed from different modes of the field, e.g., different frequencies or different k vectors, a regime exists where the existence of three possible stable output states (i.e., tristability) for a given value of the input field may occur. Using equal-amplitude input fields Walls *et al.*[4] have shown that random fluctuations of the cavity fields make the third stable branch accessible.

Incorporating additional features into the model (e.g., degeneracies) have been shown by Hermann and Thompson[8,9] to produce further stable branches. In general, the greater the order of nonlinearity associated with the driving terms, the greater will be the possibility of finding additional stable branches.

II. INTRACAVITY TWO-PHOTON ABSORPTION

The simplest model of two-photon absorption inside a cavity ignores the Stark shifts and adopts the paraxial approximation as well as the mean-field limit, defined as $\alpha L \to 0$, $T \to 0$, $C = \alpha L / T$ constant (α is the linear absorption, L the active cavity length, $T = 1 - R$ the transmissivity of the mirrors, and C is the cooperativity parameter). Omission of the Stark terms represents a somewhat drastic assumption in the purely absorptive regime (where the dispersive component of the complex susceptibility is negligibly small); however in the dispersive regime, where the net two-photon detuning Δ satisfies $\Delta^2 >> 1$, such an omission is more tolerable. As the essential physical features that we wish to study are already present in the Stark-free model, and moreover can be treated analytically in this case, we prefer to omit Stark terms in the present paper. The coupled steady-state equations that we will investigate are

$$Y_k^2 = X_k^2 \left[\left[1 + \frac{C X_l^2}{1 + \Delta^2 + X_1^2 X_2^2} \right]^2 + \left[\phi_k - \frac{C \Delta X_l^2}{1 + \Delta^2 + X_1^2 X_2^2} \right]^2 \right], \quad k, l (\neq k) = 1, 2 \tag{1}$$

where $Y_{1,2}$ are the (suitably scaled) input-field amplitudes, and $X_{1,2}$ are the corresponding output amplitudes, while $\phi_{1,2}$ are the cavity detunings for each field (in the absence of the other). These equations have been derived in various ways by a number of authors.[10–14] The experimental arrangement employs either a Fabry-Perot or a ring cavity, with two incident beams (frequencies ω_1 and ω_2) which are two-photon resonant with atoms in the cavity. We restrict ourselves to considering only the fundamental spatial harmonics in the Fabry-Perot case, so that Eqs. (1) do not accurately account for the full complement of standing wave effects in this case.

Considerable simplifications occur when we set $Z_k = Y_k^2(1+\Delta^2)^{-1/2}$, $U_k = X_k^2(1+\Delta^2)^{-1/2}$, and $D = C(1+\Delta^2)^{-1/2}$ in Eqs. (1):

$$Z_k = U_k\left[\left[1+\frac{DU_l}{1+U_1U_2}\right]^2 + \left[\phi_k - \frac{D\Delta U_l}{1+U_1U_2}\right]^2\right]. \tag{2}$$

It will be noticed immediately that there are two orders of nonlinearity in these equations. Thus Eqs. (2) as they stand are *strongly* nonlinear, while for $U_1U_2 << 1$ we have to consider the *weakly* nonlinear form

$$Z_k = U_k[(1+DU_l)^2+(\phi_k - D\Delta U_l)^2]. \tag{3}$$

The constraint $U_1U_2 << 1$ is precisely the condition that the atoms should be far from saturation (with respect to the populations of the initial and final atomic states).

The conditions for various types of multistability may be elucidated by performing a linear stability analysis on the Maxwell-Bloch equations governing the dynamics of the two-photon processes (see also discussion in the Appendices).

Although the problem in its generality requires a linearization of seven dynamical variables about the steady state, it was shown in Ref. 2 that the "good-cavity" limit (where atomic variables relax to their steady-state values much faster than field variables) involves only four field variables, and that the case $\Delta = \phi_k = 0$ reduces this number still further to two. The deterministic differential equations formed by adiabatic elimination of the atomic variables are, in the mean-field model,

$$\kappa^{-1}\frac{d\hat{E}_k}{dt} = \hat{E}_{k0} - \hat{E}_k[1+\chi_{1k} + i(\phi_k - \chi_{2k})], \tag{4}$$

where $\chi_k = \chi_{1k} - i\chi_{2k}$ is the intensity-dependent susceptibility of the kth field, κ^{-1} is the cavity decay time, $\hat{E}_k = X_k(t)e^{i\phi_k(t)}$ are the (complex) transmitted fields and $\hat{E}_{k0} = Y_k e^{i\theta_k}$ are the incident fields. Consistent with Eqs. (2), $\chi_{1k} = DU_l/(1+U_1U_2)$ and $\chi_{2k} = D\Delta U_l/(1+U_1U_2)$. Some analytical results arising from a simplified stability analysis of Eq. (4) are shown in Appendix A. As the case $\Delta = \phi_k = 0$ can be handled analytically much more easily than other cases, we will discuss this first. We will then extend the model to include nonzero Δ and ϕ_k, in particular for the equal-input field situation ($Y_1 = Y_2$, $\theta_1 = \theta_2$, $\phi_1 = \phi_2$).

III. UNEQUAL INPUT AMPLITUDES ($Y_1 \neq Y_2$)

In Ref. 2 it is established that Stark-free ($\sigma_k = 0$) resonant two-photon optical bistability with two distinct driving fields possesses (in the good-cavity case) a (2×2) stability matrix $\hat{M}$, and that the sole criteria for stability are $\mathrm{tr}\hat{M} > 0$ and $\det\hat{M} > 0$. When Y_2 is held constant, with Y_1 varying over the domains of interest, the second inequality reduces to

$$\frac{dY_1}{dX_1}\frac{\partial Y_2}{\partial X_2} = -\frac{dY_1}{dX_2}\frac{\partial Y_2}{\partial X_1} > 0 \tag{5}$$

enabling the domains of stability and instability in the steady-state curves to be mapped out with ease. Domains of monostability, bistability, and tristability have been found for various values of C and Y_2, and the competing mechanisms in these various forms of multistability have been elucidated.[3] Competition between the reaction fields associated with the two-photon enhanced Kerr effect [the weakly nonlinear terms in Eq. (3)] provides the mechanism for bistable behavior by interactive mode pulling. A third stable state satisfying $X_1X_2 >> 1$ also occurs when the strongly nonlinear effects are taken into account. This saturation state can compete with each of the two unsaturated states, thereby generating tristability.

We have made a numerical study of two-photon optical bistability in the absorptive regime ($\Delta = \phi_k = \sigma_k = 0$), and have mapped out the different types of multistability into areas on a two-dimensional phase diagram. For convenience we have taken the two parameters defining this space to be C and $(\frac{1}{2}Y_2)^2$, with the parameter Y_1 varying over the regions of interest, and find five basic domains within which the following behavior may

be observed:

I. Monostable only;
II. Kerr bistable (two unsaturated states competing);
III. Tristable (two unsaturated and one saturated state competing together);
IV. Bistable (saturated state competing *separately* with unsaturated states);
V. Bistable (only one unsaturated state competing with saturated state).

These regions are indicated in Fig. 1.

Note the existence of a critical point P, at which all of the phases can coexist simultaneously. Subdomain IIIA is "weakly bistable" in the sense that a saturation state with a very short metastable lifetime can occur (when Y_2 is slightly smaller than $2\sqrt{C}$), which is inaccessible to the two unsaturated branches other than by chance fluctuations. The other subdomains, also occuring for Y_2 slightly smaller than $2\sqrt{C}$, indicate the existence of a hysteresis cycle involving the saturation state with the unsaturated state (that is to say, the existence of an S-shaped solution in the transmission characteristic). The line $C=2$ can be interpreted as a lower threshold for both Kerr bistability and for tristability. The line $C=(\frac{1}{2}Y_2)^2$ is an asymptote for the transition from Kerr bistability to tristability, and represents the transition stage between a single, continuous steady-state curve, and two completely separate steady-state transmission curves. When $C<(\frac{1}{2}Y_2)^2$ we find that $X_2(Y_1)$ is confined to

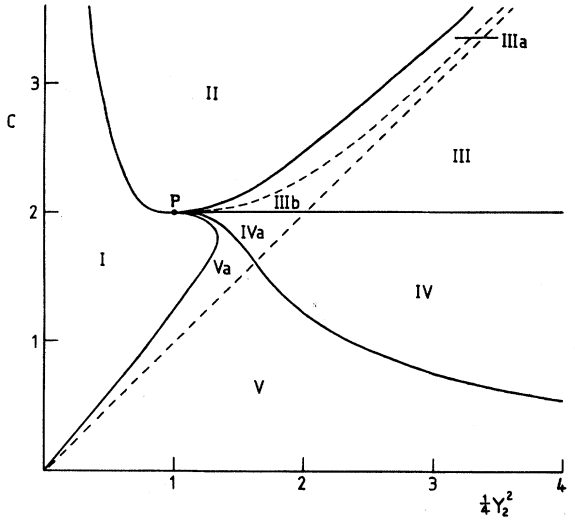

FIG. 1. The phase diagram in the parameter space C, $\frac{1}{4}Y_2^2$ (for all values of Y_1). The regions denoted I–V are described in the text, and point P is a "critical point" at which all of the phases coexist.

domains (Y_2,X_2^+) and $(X_2^-,0)$, where $X_2^{\pm}=\frac{1}{2}Y_2\pm[(\frac{1}{2}Y_2)^2-C]^{1/2}$: the gap (X_2^+,X_2^-) contains no solutions. Some examples of $X_2(Y_1)$ for different values of C and $Y_2=4$ are given in Fig. 2 (the stable branches correspond to those regions of curves where $dY_1/dX_2<0$). Note in particular that for $C=(\frac{1}{2}Y_2)^2$ the domain (X_2^+,X_2^-) has reduced to the single line $X_2=\frac{1}{2}Y_2$.

Although we have specified the mechanisms for two-photon optical bistability (Kerr effect and saturation) and for tristability, no indication of

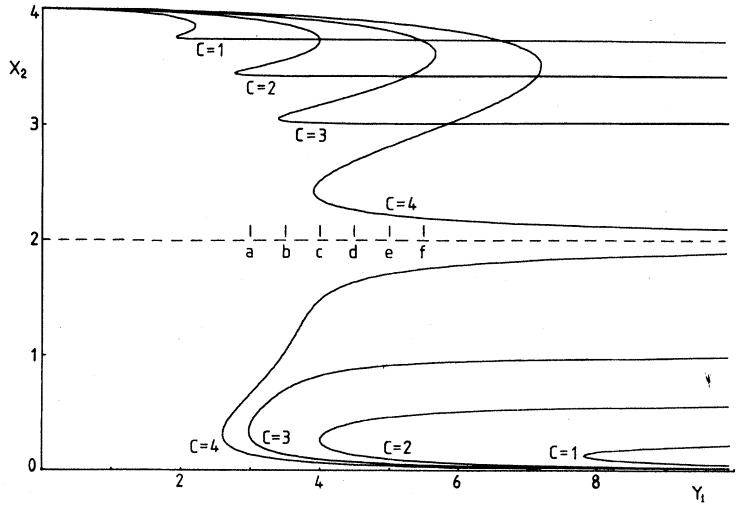

FIG. 2. Diagrams of $X_2(Y_1)$, for $Y_2=4$ and various values of C. The values of Y_1 marked a, b, c, d, e, and f, correspond to probability distributions shown in Fig. 3. Note that a single asymptote at $X_2=2$ separates the upper and lower subdomains in the case $C=4$.

which state actually wins out in a particular competitive situation has been given. In order to gain some insight into this problem, as well as into the stability problem in general, we have investigated the potential function $U(X_1,X_2)$ defined by $\kappa^{-1}dX_k/dt=-\partial U/\partial X_k$. Apart from an arbitrary constant this takes the form

$$U(X_1,X_2)=\tfrac{1}{2}[(X_1-Y_1)^2+(X_2-Y_2)^2]+\tfrac{1}{2}C\ln(1+X_1^2X_2^2). \quad (6)$$

The phases accompanying X_k and Y_k are assumed to be locked together here, while a more general phase-dependent potential is given in Appendix B. As has been shown in Ref. 4, where random field fluctuations occur within the cavity a random electric "force" term $\eta(t)$ satisfying $\langle\eta(t)\rangle=0$, $\langle\eta(t)\eta(t')\rangle=\delta(t-t')$ should be added to the time-dependent field equations. A time-dependent probability distribution $P(X_1,X_2,t)$ satisfying the Fokker-Planck equation can be constructed, and its stationary form is generally proportional to $\exp[-\beta_0 U(X_1,X_2)]$, where β_0 determines the scale of the fluctuations. In Fig. 3 we show $e^{-U(X_1,X_2)}$ for increasing values of the input field Y_1, choosing $C=3$ and $Y_2=4$ (i.e., within the tristable domain). The corresponding points in the $X_2(Y_1)$ graph are indicated in Fig. 2. The three states, represented by the maxima of the peaks, clearly have comparable heights within a narrow range of values of $Y_1(\sim 4.0)$, and thus comparable metastable lifetimes. This represents a strongly tristable situation, and is to be contrasted with the situation (described in Ref. 2) encountered in the case $Y_2=C=4$, wherein the intermediate (saturation) state always possesses a probability peak much smaller than the peaks representing the unsaturated states, although it remains directly accessible to both unsaturated states as can be verified by constructing an extremum path.

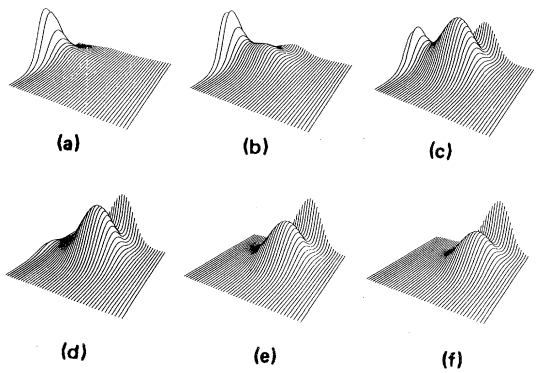

FIG. 3. The two-photon probability distributions function $P(X_1,X_2)=\exp[-U(X_1,X_2)]$ for increasing Y_1 values: (a) $Y_1=3.0$, (b) $Y_1=3.5$, (c) $Y_1=4.0$, (d) $Y_1=4.5$, (e) $Y_1=5.0$, (f) $Y_1=5.5$. Other relevant parameters are $C=3$ and $Y_2=4$.

Only the saturation states encountered in subdomain IIIA are truly inaccessible in terms of switching processes taking place between the unsaturated states. It is of interest to determine for given Y_1, Y_2, and C, the relative lifetimes of the metastable branches. This is generally difficult, although some special cases can be evaluated. For example, where we may assume that $X_1=Y_1$, there are two possible states: (a) the second unsaturated state, for which $X_2<<Y_2$; (b) the saturation state, for which $X_2\simeq Y_2$. The approximate potential function

$$U\simeq\tfrac{1}{2}(X_2-Y_2)^2+\tfrac{1}{2}C\ln(1+Y_1^2X_2^2)$$

reduces in case (a) to $U\simeq\frac{1}{2}(X_2-Y_2)^2+\frac{1}{2}CY_1^2X_2^2$. The minima of the states are approximately (a) $\frac{1}{2}Y_2^2$ and (b) $\frac{1}{2}C\ln(1+Y_1^2Y_2^2)$, hence for the stable unsaturated state we have $Y_2^2<C\ln(1+Y_1^2Y_2^2)$ and for the stable saturation state $Y_2^2>C\ln(1+Y_1^2Y_2^2)$. These results demonstrate that for given Y_1 and Y_2 there is a special value of C ($\simeq Y_2^2/\ln(1+Y_1^2Y_2^2)$ in the above example) for which the potential wells corresponding to the upper (second) unsaturated state and the saturation state are of equal depth. The case of comparable metastable lifetimes for the saturated and unsaturated states discussed above and plotted in Fig. 3(c) ($Y_1\simeq Y_2\simeq 4$, $C\simeq 3$) corresponds to this special value of C.

An alternative, and in some ways more general, phase diagram can be constructed by placing the input fields Y_1, Y_2 on an equal footing with respect to the multistable domains. Thus, we can construct the volume domains in (C,Y_1,Y_2) — space for each of the types of multistable behavior in isolation. The contour profile diagram in (Y_1,Y_2) for increasing values of C is very complicated, and consequently we have found it expedient to plot the various cross sections for $C=1$, 2, 4 separately (see Fig. 4). The various domains in these cross sections can be related to the corresponding domains in Fig. 5. A feature which emerges most clearly in these cross sections is the symmetrical disposition of the two domains of bistability representing competition between the saturation state and each of the unsaturated states separately (designated as B_1 and B_2). It must be concluded that there is no essential difference in nature between the bistable mechanisms character-

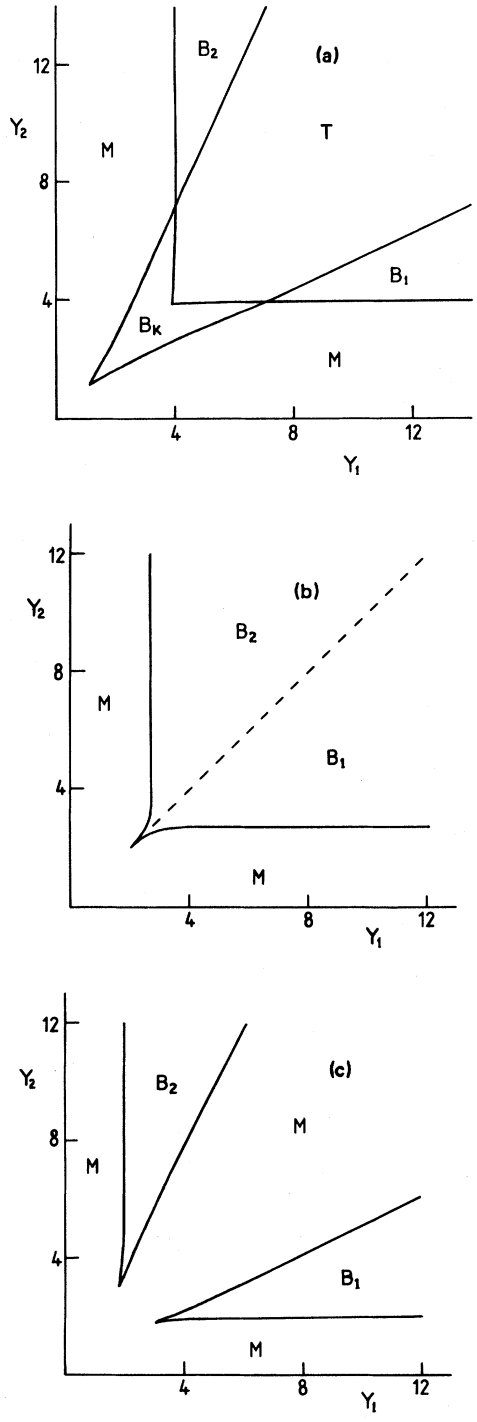

FIG. 4. Cross sections of the multistability phase diagram in parameter space C, Y_1, Y_2 taken at values (a) $C=4$, (b) $C=2$, and (c) $C=1$. At $C=2$, the Kerr bistable region B_k is reduced to a line, and ceases to exist when $C<2$. The saturation bistable domains B_1, B_2 are mirror images about the $Y_1=Y_2$ line. Monostable regions are designated M and tristable regions T.

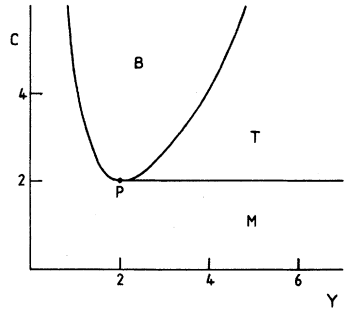

FIG. 5. The phase diagram in C, Y space, for the special case $Y_1=Y_2=Y$. The monostable region is designated M, bistable B, and tristable T, while P is a critical point.

izing regions B_1 and B_2. All monostable regions (designated M) are likewise equivalent. In the graph for cross section $C=4$ we see that the tristable region (designated T) represents a common area in the overlap of the unsaturated bistable region (designated B_k) and the saturation-bistable region (B_2+B_1). At $C=2$ it will be observed that the unsaturated region B_k reduces to a single line $Y_1=Y_2$, while for $C<2$ the region B_k does not exist and regions B_1, B_2 separate from each other (B_1 is the mirror image of B_2 about the line $Y_1=Y_2$). The plane through $Y_1=Y_2$ for varying C clearly is a very special case, and the properties of the equations of state when $Y_1=Y_2$ will receive detailed study in the next section. However, we can infer that domains IV and V are absent from the phase diagram for C and $Y(=Y_1=Y_2)$, and we have plotted this special phase diagram in Fig. 5. Fluctuations of Y_1 and Y_2 will always be present in reality, and deviations from the $Y_1=Y_2$ plane can take the system into the adjacent B_1, B_2, and B_1+B_2 regions.

IV. EQUAL-INPUT AMPLITUDES ($Y_1=Y_2=Y$)

The steady-state description of the equal-input amplitudes case ($Y_1=Y_2$) has been investigated by Walls *et al.*[4,5] for the special situation $\Delta=\phi_k=0$. This analysis may be extended to include nonzero Δ and ϕ_k as follows. Equating Eqs. (2) we find that when $\phi_1=\phi_2$ ($=\phi$) there are two solutions:

$$Z=\frac{Y^2}{(1+\Delta^2)^{1/2}}=U_1\left[\left[1+\frac{DU_1}{1+U_1^2}\right]^2+\left[\phi-\frac{D\Delta U_1}{1+U_1^2}\right]^2\right] \quad \text{for } X_1=X_2 \tag{7a}$$

$$Z=\frac{Y^2}{(1+\Delta^2)^{1/2}}=U_1\left[\left[1+\frac{\lambda}{U_1}\right]^2+\left[\phi-\frac{\Delta\lambda}{U_1}\right]^2\right] \quad \text{for } X_1\neq X_2$$

$$U_1U_2=\frac{\lambda^2}{1+\phi^2}, \tag{7b}$$

with λ taking the two values

$$\lambda=\lambda_{\pm}=\tfrac{1}{2}C\pm[(\tfrac{1}{2}C)^2-(1+\phi^2)]^{1/2}. \tag{8}$$

In order to have three distinct curves $Z(U_1)$ for all X_1, X_2 it is necessary that $C>2(1+\phi^2)^{1/2}$. The turning points in the two curves for $X_1\neq X_2$ are (U_1^s,Z^s), where

$$\begin{aligned} U_1^s&=\lambda(1+\phi^2)^{-1/2},\\ Z_1^s&=2\lambda[(1+\phi^2)^{1/2}\\ &\quad+(1-\phi\Delta)(1+\Delta^2)^{-1/2}]. \end{aligned} \tag{9}$$

We may label these quantities with a $\pm$ suffix for specific values of λ. These two sets of points are also *bifurcation points,* as well as *crossing points* for the curve corresponding to $X_1=X_2$ [case (7a)]. We can demonstrate first that the points are crossing points by equating Eqs. (7a) and (7b), whereupon the solutions $U_1=U_1^s$ are found. Apparent crossing points also appear for sufficiently large detunings. These are not true crossing points however, but are merely projections onto a plane cutting the Δ axis, and reflect the multiparameter nature of the equations of state (see the later discussion). In Figs. 6(a)–6(c) we show the effect of increasing C beyond the multistability threshold $C=2$ (at which point the two curves corresponding to $X_1\neq X_2$ coincide, and below which the system is monostable only). Also, in Fig. 6(c) we show that for a relatively large value of Δ the turning points remain crossing points, and that additional "apparent" crossing points have appeared.

In order to establish that the two points (U^s,Z^s) are bifurcation points, we return to the stability criteria for the equation of state (7a). In the case $\Delta=\phi_k=0$ we find

$$\mathrm{tr}\hat{M}=\frac{2Y}{X}-\frac{4CX^6}{(1+X^4)^2}>0,$$

$$\det\hat{M}=\left[\frac{Y}{X}-\frac{2CX^6}{(1+X^4)^2}\right]^2-\frac{4C^2X^4}{(1+X^4)^4}>0,$$

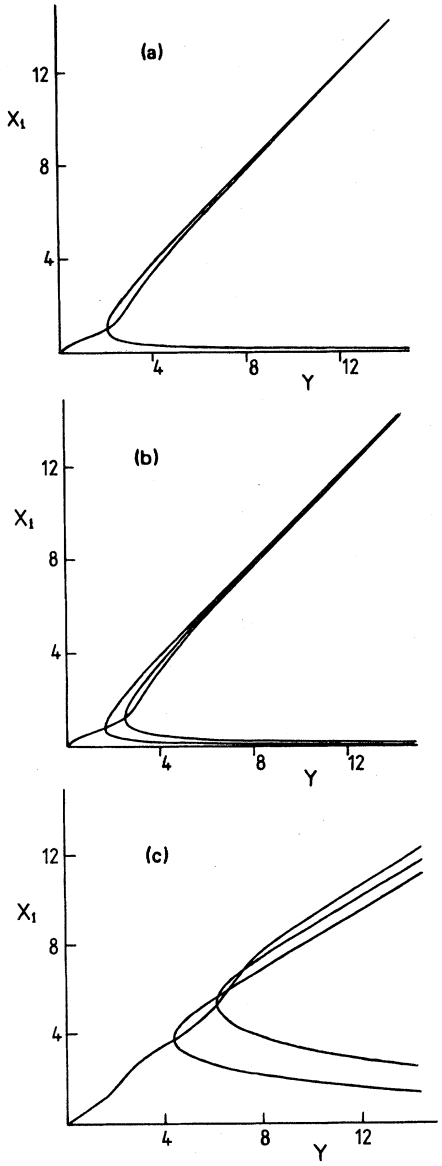

FIG. 6. Transmission characteristics for $Y_1=Y_2=Y$; input amplitude Y vs output amplitude X_1 for values (a) $C=2.0$, $\Delta=\phi=0$, (b) $C=2.2$, $\Delta=\phi=0$, (c) $C=3$, $\Delta=10$, $\phi=1$. When interpreting these diagrams we note that $n-1$ unstable states accompany n-fold multistability.

where $X_1=X_2=X$.

Reconciling these inequalities and simplifying, we have the result

$$(X^2-\lambda_+)(X^2-\lambda_-)>0.$$

This indicates that the domain of instability for the $X_1=X_2$ curve is $\lambda_-^{1/2}<X<\lambda_+^{1/2}$. A similar analysis in the $X_1\neq X_2$ case also reveals that the outermost curve [corresponding to $\lambda=\lambda_-$ in Eq. (7b)] is stable, while the conjugate inner curve ($\lambda=\lambda_+$) is unstable. Hence tristability can occur when $Z>Z_+^s$, with bistability for $Z_-^s<Z<Z_+^s$ and monostability for $Z<Z_-^s$. The corresponding arguments in the more general case in which dispersive components are present will be left in detail to a subsequent publication.

Further light is thrown upon these matters by studying the structural stability of the Eqs. (1) with respect to small perturbations about $Z_1=Z_2$. To this end we can linearize the problem in the form $Z_1=Z_2+\epsilon$, with ϵ a small perturbation. Thus, it is convenient to set $\phi_1=\phi_2=\phi$ in Eqs. (2) and to set

$$U_1=U_0(U_2)+\epsilon H(U_2)+O(\epsilon^2). \tag{10}$$

Using Eqs. (2) in conjunction with (10) we can evaluate $\epsilon=Z_1-Z_2$; equating coefficients of ϵ, it follows that

$$\begin{aligned}H(U_2)^{-1}=&\left[1+\frac{DU_2}{1+U_0U_2}\right]^2+\left[\phi-\frac{D\Delta U_2}{1+U_0U_2}\right]^2\\&-\frac{2DU_2}{(1+U_0U_2)^3}[DU_0(1+\Delta^2)+(1+U_0U_2)(1-\Delta\phi)]\\&-\frac{2DU_0U_2^2}{(1+U_0U_2)^3}[DU(1+\Delta^2)+(1+U_0U_2)(1-\Delta\phi)]\,.\end{aligned} \tag{11}$$

The singularities in $H(U_2)$ (if any) are determined by solving the polynomial equation formed by equating the right-hand side of Eq. (11) to zero. In the case $U_2=U_0(=U)$ we find $U=\lambda(1+\phi^2)^{-1/2}=U_s$, and the case $U_2\neq U_0$ can also be solved with somewhat more difficulty to yield again $U=U_s$. It is significant that the linear analysis breaks down only at the two crossing points, indicating that these are bifurcation points while the "apparent" crossing points are clearly not bifurcation points.

V. EFFECTS OF THE DETUNINGS UPON TRANSMITTED AMPLITUDES

The equation of state for single-photon-resonant optical bistability in a Fabry-Perot cavity has been thoroughly explored in the mean-field dispersive and absorptive regimes by Agrawal and Carmichael,[15] and also by Carmichael and Hermann[16] where spatial effects are fully accounted for (proper treatment of standing waves). Corresponding studies of dispersive bistability in a ring cavity have been reported by a number of other authors.[17–19] The behavior of these multiparameter steady-state equations, in particular the aspects of switching and hysteresis, can be understood on the basis of the format of catastrophe theory.[15] Some interesting behavior occurs when the input-field amplitude and phase is held fixed and the detunings of the atoms and of the cavity are varied; in Ref. 16 it is shown that in these circumstances a succession of bistability "islands" (which may or may not exhibit hysteresis) occur as the input amplitude is successively increased. We will show that similar behavior occurs in the two-photon system and for simplicity of analysis we consider only the case of $Y_1=Y_2$. It will be noticed that Eqs. (7a) and (7b) may be regarded as equations for U_1 as a function of Δ and ϕ with Y fixed, and we have therefore plotted the curves $X_1(\Delta)$ for $C=3$, $Y=4$ in Figs. 7(a) and 7(b). The graphs exhibit pitchfork bifurcations and domains of mono-, bi-, and tristability. Considerable distortions occur as ϕ changes from zero to unity. Note that the crossing points of the $X_1=X_2$ and $X_1\neq X_2$ curves are once again turning points and bifurcation points, similar in nature to those found in the $X(Y)$ curves. The basic difference is that Δ may take negative as well as positive values, leading to multistability islands similar in nature to those found in the single-photon-resonant counterparts. In all cases it can be shown analytically that $\partial X_1/\partial\Delta$ is zero at $\Delta=0$.

An alternative procedure is to plot X_1 as a function of ϕ for fixed Δ, C, and Y. In Fig. 8 we show

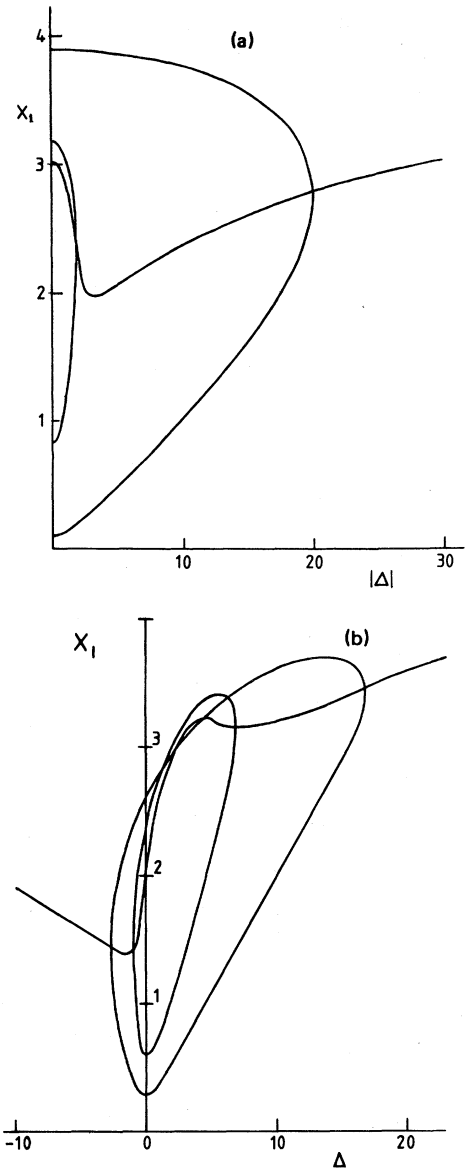

FIG. 7. The curves $X_1(\Delta)$ for $C=3$, $Y=4$ ($Y_1=Y_2=Y$ and $\phi_1=\phi_2=\phi$) with (a) $\phi=0$, (b) $\phi=1$. In case (a) the curves are symmetric about the X_1 axis, and only positive values of Δ are shown.

$X_1(\phi)$ for $\Delta=0$, $C=3$, $Y=4$ and the islands of tristability are clearly evident for the domain $1+\phi^2<(\frac{1}{2}C)^2$. If $X_1(Y)$ is confined solely to the intermediate branch (the "saturation" branch), then we can plot the crossing points X_{1s} as functions of ϕ with the other parameters fixed. This is shown in Fig. 9, from which it can be seen that the upper and lower points join smoothly at $1+\phi^2=(\frac{1}{2}C)^2$, creating *areas* of multistability. Another alternative is to construct the domains of multistability in

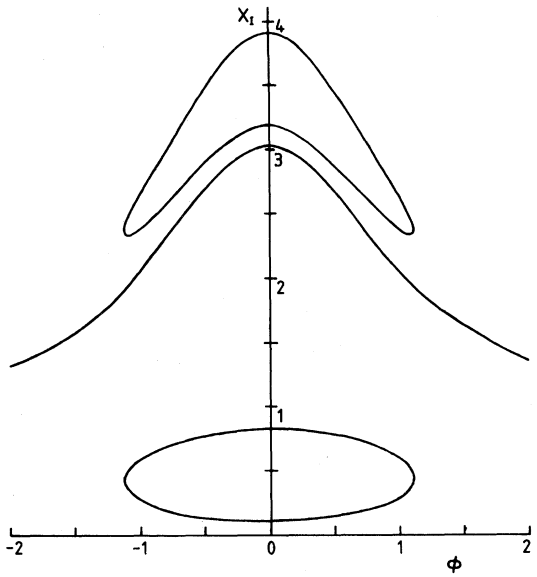

FIG. 8. The curves $X_1(\phi)$ for $C=3$, $Y=4$ ($Y_1=Y_2=Y$ and $\phi_1=\phi_2=\phi$) with $\Delta=0$.

the $\phi-\Delta$ plane for fixed C and Y, in analogy to the single-photon domains given in Refs. 15–17. In this case it is sufficient to differentiate the equations of state (7b) for the conjugate branches.

From Equations (9) we have the turning points given by $\partial Y/\partial X_1=0$ as

$$Y_{\pm}^2=2\lambda_{\pm}\{[(1+\phi^2)(1+\Delta^2)]^{1/2}+1-\phi\Delta\}$$

and the multistable regimes are represented by the inequalities:

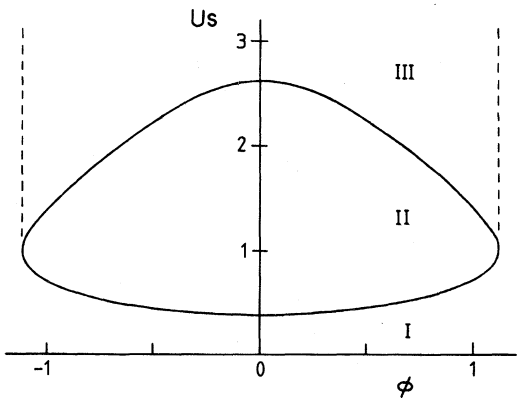

FIG. 9. Crossing points X_{1s} on the saturation branch of $X_1(Y)$, plotted as $U_s=X_{1s}^2$ vs ϕ, with the other parameters fixed ($C=3$, $\Delta=0$). The adjacent domains I–III in $U(=X_1^2)$, ϕ space are mono-, bi-, and tristable, respectively.

(a) Monostable $Y < Y_-$;
(b) Bistable $Y_- < Y < Y_+$;
(c) Tristable $Y > Y_+$.

We have plotted the boundaries of these domains ($Y = Y_\pm$) in Fig. 10 for representative values of Y and C. Alternatively, the turning points given by $\partial\Delta/\partial X_1 = 0$ again give the multistability boundaries as $Y = Y_\pm$. All of these cross sections in the hyperspace of parameters Y, C, Δ, ϕ (and more generally parameters Y_1, Y_2, C, Δ, ϕ_1, ϕ_2) highlight the complexity of the complete phase diagram for the multistable domains.

VI. CONCLUSIONS

An analysis of an intracavity two-photon absorber interacting with two coherently driven cavity modes has been given. The possible stable output configurations of the cavity modes were determined. For weak driving fields (unsaturated medium) two stable output states are possible. For higher values of the driving field (saturated medium) a third possible stable state exists. Competition between these states results in regions of bistable and tristable behavior.

In the purely absorptive case the domains of stability are determined as functions of the driving-field amplitudes Y_1 and Y_2 and the cooperativity parameter C. In this case a steady-state solution for the probability distribution of the mode amplitudes exists. This enabled the relative lifetimes of the metastable branches to be deduced. In the dispersive situation a linearized stability analysis was required. The domains of stability were determined as of function of C, the cavity and atomic detunings ϕ and Δ, and the driving-field amplitude Y (where we have chosen $Y_1 = Y_2$). This analysis reveals the rich variety of behavior that may occur in this two-mode multiparameter system.

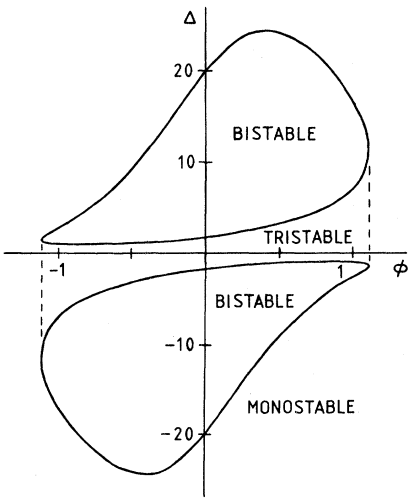

FIG. 10. The domains of multistability in the ϕ-Δ plane, given by $Y = Y_\pm$, with parameter values $C = 3$, $Y = 4$.

ACKNOWLEDGMENT

Assistance given by Mr. C. Penman, of the laser theory group at Imperial College, in plotting Figs. 3(a)–3(f) is gratefully acknowledged. The research reported here has been supported in part by the United States Army through its European Research Office.

APPENDIX A

A general linear stability analysis of two-photon optical multistability and bifurcations is very complicated, particularly when two field modes are involved in the two-photon resonance and when Stark terms are included in the equations of motion (an indication of the level of complexity is provided in Ref. 2). However, considerable insight as well as analytic solutions can be extracted by restricting the model in various ways. As a guide to this process, we can make use of the stability analyses of the two-level homogeneously broadened model of single-photon-resonant optical bistability. As well as showing that regions in the $Y(X)$ curves with negative slope are unstable, these studies clearly show that instabilities of the self-pulsing type can be expected in the saturation branch[18,20–23] and can be explained in terms of coupling between adjacent cavity modes. We would not expect cavity modes other than the resonant mode to be relevant to the dynamics of two-photon *unsaturated* Kerr bistability, and therefore the mean-field model should suffice in this case. We also note that recent investigations of self-pulsing in dispersive bistability by Lugiato[21] appear to show that this phenomenon can be expected to be virtually absent from a purely dispersive system (for which the essential requirements are $\Delta^2 \gg 1$, $\phi\Delta \gg 1$, $\phi/\Delta \ll 1$), and it is reasonable to anticipate similar behavior with regard to the two-photon saturation branch. Two-photon optical bistability experiments have hitherto been restricted to this regime.[7]

The appropriate stability matrix for two-field modes can be derived by linearizing Eq. (4) about the steady state. In this connection we intend to explore only bistable behavior between the unsaturated states of the system. Stark terms are once again ignored. In drawing attention to this regime, we emphasize that tristability arises when bistability by the unsaturated Kerr mechanism competes with bistability by the two-photon bleaching mechanism, and that stability aspects of the latter have already been discussed.[12] Writing $\hat{E}_k = X_{ka} + iX_{kb}$, $|\hat{E}_k| = X_k$ we find that the stability matrix $\hat{M}$ can be easily calculated upon separating real and imaginary parts of Eq. (4) and applying standard procedures,[24] yielding

$$\hat{M} = \begin{bmatrix} -\lambda_1 & \xi_1 & a+\Delta b & c+\Delta d \\ -\xi_1 & -\lambda_1 & b-\Delta a & d-\Delta c \\ a+\Delta c & b+\Delta d & -\lambda_2 & \xi_2 \\ c-\Delta a & d-\Delta b & -\xi_2 & -\lambda_2 \end{bmatrix}, \tag{A1}$$

where, for unsaturated states only, we find

$$\lambda_k = 1+\bar{D}X_l^2, \quad \xi_k = \phi_k - \bar{D}\Delta X_l^2, \quad l\ (\neq k) = 1,2$$

$$\bar{D} = C/(1+\Delta^2)$$

$$a = -2\bar{D}X_{1a}X_{2a}, \quad b = -2\bar{D}X_{1b}X_{2a}, \quad c = -2\bar{D}X_{1a}X_{2b}, \quad d = -2\bar{D}X_{1b}X_{2b}.$$

These parameters also could be calculated to higher orders of the nonlinearity to allow the full complement of multistable effects to be studied. The general aim is to determine conditions for which the real parts of the eigenvalues of $\hat{M}$ are all negative, thereby satisfying the criterion for stability. We will discuss two extreme cases.

(1) In the purely absorptive case ($\Delta = \phi_k = 0$) $\hat{M}$ is effectively 2×2 and there are only two eigenvalues,

$$\mu_{1,2} = -1 + \tfrac{1}{2}\bar{D}\{-(X_1^2+X_2^2) \mp [(X_1^2+X_2^2)^2 + 12X_1^2X_2^2]^{1/2}\}. \tag{A2}$$

Where $X_1 = X_2$, we find that (A2) provides the stability conditions for two different physical situations: (a) for the field-degenerate case the equation of state is $Y = X + \bar{D}X^3$ and we have $\mu_1 = -dY/dX = -(1+3\bar{D}X^2)$, indicating only monostability; (b) for the nondegenerate case with $Y_1 = Y_2\ (=Y)$, we find two branches of $Y(X_1)$ corresponding to $X_1 \neq X_2$ and $X_1 = X_2$, respectively. The eigenvalue $\mu_2 = \bar{D}X_1^2 - 1$ indicates that the $X_1 = X_2$ branch is unstable when $\bar{D}X_1^2 > 1$. Simple analysis of the equations of state reveals that the point on $Y(X_1)$ where $\bar{D}X_1^2 = 1$ is both a branch crossing point and a minimum of the $X_1 \neq X_2$ branch.

(2) The purely dispersive case corresponds to setting $\lambda_k = 1$ in (A1) and retaining only terms proportional to Δ in the off-diagonal submatrices. The four eigenvalues $\mu_{\eta,\epsilon}$ satisfying $\det(\hat{M} - \mu I) = 0$ are given by

$$\mu_{\eta,\epsilon} = -1 + \eta[-\theta + \epsilon(\theta^2+\varphi)^{1/2}]^{1/2}, \quad \theta = \tfrac{1}{2}(\xi_1^2+\xi_2^2)$$

$$\varphi = \xi_1\xi_2(a^2+b^2+c^2+d^2-\xi_1\xi_2), \quad \eta = \pm 1, \quad \epsilon = \pm 1. \tag{A3}$$

This simple result has been made possible by virtue of the property that the determinants of the off-diagonal submatrices (in this case *ad-bc*) vanish identically. Note that this property is quite general for a two-photon system. Pertinent to Sec. IV is the case where $\phi_1 = \phi_2\ (=\phi)$ and $U_1 = U_2\ (=U)$; here $\xi_1 = \xi_2$ and (A3) becomes

$$\mu_{\eta,\epsilon} = -1 + \eta[\bar{D}^2U^2 - (\phi - \bar{D}U + \epsilon\bar{D}U)^2]^{1/2}. \tag{A4}$$

The two sets of signs in (A4) are independent; furthermore the eigenvalue subsets corresponding to $\epsilon = +1$ and $\epsilon = -1$ describe different physical situations, as in the absorptive case. Thus the eigenvalues with $\epsilon = -1$ provide the stability condition for the degenerate two-photon dispersive system. Here the equation of state is

$$Z = U[1 + (\phi - \bar{D}\Delta U)^2]$$

and equation (A4) becomes

$$\mu_{\eta,-} = -1 + \eta\left[1 - \frac{\partial Z}{\partial U}\right]^{1/2}.$$

Where $\epsilon=+1$, we are again concerned with identifying the bifurcation point of the nondegenerate case with $Z_1=Z_2$ $(=Z)$, thus

$$\mu_{\eta,+}=-1+\eta(\bar{D}^2U_1^2-\phi^2)^{1/2}$$

indicates that stability in the $U_1=U_2$ branch ceases when $\bar{D}^2U_1^2>1+\phi^2$, and the point in $Z(U_1)$ where $\bar{D}^2U_1^2=1+\phi^2$ is easily shown to be both a crossing point and a minimum.

APPENDIX B

The deterministic two-photon potential $U(X_1,X_2)$ of Eq. (6) is a function of the field amplitudes only, in accordance with the assumption that the phases φ_k and θ_k are always locked together. More generally, Eq. (4) can be expressed as as the set of equations

$$\kappa^{-1}\frac{dX_k}{dt}=-\frac{\partial U}{\partial X_k}, \tag{B1}$$

$$\kappa^{-1}\frac{d\varphi_k}{dt}=-X_k^{-2}\frac{\partial U}{\partial \varphi_k};\quad k=1,2 \tag{B2}$$

with the potential function

$$U(X_1,X_2,\varphi_1,\varphi_2)=\tfrac{1}{2}(X_1^2+X_2^2)+\tfrac{1}{2}C\ln(1+X_1^2X_2^2)$$
$$-X_1Y_1\cos(\varphi_1-\theta_1)-X_2Y_2\cos(\varphi_2-\theta_2). \tag{B3}$$

If one wishes to make a quantitative prediction, it will be necessary to integrate over the phases in accordance with the above equations. Thus, for the same value of C and the same set of input amplitudes, the relative weights of the branches can differ markedly from those calculated under the simplifying assumption that the phases are strongly locked onto their deterministic values (see Sec. III). The qualitative predictions are identical however (information to this effect derived from numerical computations by Mr. C. Savage is acknowledged).

[1]M. Kitano, T. Yabuzaki, and T. Ogawa, Phys. Rev. Lett. 46, 926 (1981).

[2]J. A. Hermann, Opt. Commun. 37, 431 (1981).

[3]J. A. Hermann, J. N. Elgin, and P. L. Knight, Z. Phys. (in press).

[4]D. F. Walls, C. V. Kunasz, P. D. Drummond, and P. Zoller, Phys. Rev. A 24, 627 (1981).

[5]D. F. Walls, C. V. Kunasz, P. D. Drummond, and P. Zoller, in *Proceedings of the International Conference on Synergetics,* edited by H. Haken (Springer, Berlin, 1981).

[6]F. T. Arrechi and A. Politi, Lett. Nuovo Cimento 23, 65 (1978).

[7]E. Giacobino, M. Devaud, F. Biraben, and G. Grynberg, Phys. Rev. Lett. 45, 434 (1980).

[8]B. V. Thompson and J. A. Hermann, Phys. Lett. 83A, 376 (1981).

[9]B. V. Thompson and J. A. Hermann, in *Proceedings of the Fifth National Quantum Electronics Conference,* edited by P. L. Knight (Wiley, New York, 1981).

[10]G. P. Agrawal and C. Flytzanis, Phys. Rev. Lett. 44, 1058 (1980).

[11]G. P. Agrawal and C. Flytzanis, in *Optical Bistability, Proceedings of the International Conference on Optical Bistability,* Asheville, North Carolina, 1980, edited by M. Bowden, M. Ciftan, and H. Robl (Plenum, New York, 1981), p. 221.

[12]J. A. Hermann and B. V. Thompson, in *Optical Bistability,* Ref. 11, p. 199.

[13]J. A. Hermann and B. V. Thompson, Phys. Lett. 79A, 153 (1980).

[14]G. S. Agarwal, Opt. Commun. 35, 149 (1980).

[15]G. P. Agrawal and H. J. Carmichael, Phys. Rev. A 9, 2074 (1979).

[16]H. J. Carmichael and J. A. Hermann, Z. Phys. B 38, 365 (1980).

[17]S. S. Hassan, P. D. Drummond, and D. F. Walls, Opt. Commun. 27, 480 (1978).

[18]R. Bonifacio and L. A. Lugiato, Lett. Nuovo Cimento 21, 505 (1978); 21, 510 (1978); 21, 517 (1978).

[19]R. Bonifacio, M. Gronchi, and L. A. Lugiato, Nuovo Cimento B53, 311 (1979).

[20]M. Gronchi, V. Benza, L. A. Lugiato, P. Meystre, and M. Sargent III, Phys. Rev. A 24, 1419 (1981) and references therein.

[21]L. A. Lugiato, Opt. Commun. 33, 108 (1980).

[22]V. Benza and L. A. Lugiato, in *Optical Bistability,* Ref. 11, p. 9.

[23]R. Bonifacio, M. Gronchi, and L. A. Lugiato, in *Optical Bistability,* Ref. 11, p. 31.

[24]H. Leipholz, *Stability Theory* (Academic, New York, 1970), p. 33.